Fourier spectroscopy of a spin-orbit coupled Bose gas

Ana Valdés-Curiel, Dimitri Trypogeorgos, Erin E. Marshall, Ian B. Spielman

Joint Quantum Institute, University of Maryland and National Institute of Standards and Technology, College Park, Maryland, 20742, USA

Abstract.

We have developed a new technique to measure the band structure of a spin-1 spin-orbit coupled Bose-Einstein condensate which relies on the time-domain evolution of the Hamiltonian. We drive transitions at different values Raman detuning and extract the frequencies from the Fourier transform of the time evolution to reconstruct the spin and momentum dependent energy spectrum. We are able to map the SOC dispersion both for time independent coupling and also for a periodically driven system, which has a tunable spin-orbit coupling dispersion and a spectrum of Floquet quasi-energies, showing the robustness of our technique.

1. Introduction

Properties of materials deeply depend in their underlying band structure. Cold atoms systems offer an exciting possibility to engineer single particle dispersions that are analogues to condensed matter systems and new exotic materials, e.g. completely flat bands where interactions dominate the system, spin-orbit systems, systems with non-trivial topology [1, 2].... The ability to measure the engineered dispersions leads to a deeper understanding and paves the way to accessing new phases of matter.

The relation between the energy spectrum of a system and its dynamics is rooted in the heart of quantum mechanics. This relation has been exploited before to study spectral properties of both condensed matter [need a good cite here] and cold atoms systems [3, 4] alike. We propose a new Fourier spectroscopy technique to measure the dispersion relation of spin-orbit coupled ultra-cold atoms, which unlike previously studied techniques [5], relies only in the time evolution of the Hamiltonian, as the bare atomic eigenstates are projected into a superposition of dressed states when a field is suddenly turned on, and proceed to evolve under that field. The spectral components of the Fourier transform then correspond to the relative energies of the dressed eigenstates.

We engineered a dispersion relation that has equal contributions of Rashba and Dresselhaus spin-orbit coupling (SOC) by coupling the different spin projections of a spin-one system laser fields [6]. We study the case of SOC driven by a single frequency, which is equivalent to a time independent problem in a rotating frame, and SOC driven by multiple frequencies, which is equivalent to periodically driven system but can be described by an effective time independent model with tunable SOC strength [7].

We generate the spin-orbit coupling using a pair of 'Raman' laser beams that change the spin state while imparting a spin-dependent momentum to a spin-one atom via two photon Raman transitions. Our system consists of ultra-cold ^{87}Rb atoms, and we use the magnetic sub-levels of the $F = 1$ ground state hyperfine manifold as different spin projections [8, 9]. A uniform magnetic field $B\hat{\mathbf{e}}_z$ generates a linear Zeeman splitting of the energy levels $\hbar\omega_Z = g_F\mu_B B$, where μ_B is the Bohr magneton and g_F is the Landé g factor, and introduces a quadratic Zemen shift ϵ that shifts the energy of the $|m_F = 0\rangle$ state with respect to the $|m_F = \pm 1\rangle$ states. We couple the three states using a pair of intersecting, cross polarized Raman beams with angular frequency ω_A and $\omega_B = \omega_A + \omega_Z + \Delta_0$, where Δ_0 is an experimentally controllable detuning from four photon resonance between the $|m_F = -1\rangle$ and $|m_F = +1\rangle$ states. The Raman field couples the state $|m_F = 0,\ q_x\rangle$ to $|m_F = -1,\ q_x + 2k_L\rangle$ and to $|m_F = +1,\ q_x - 2k_L\rangle$, generating a spin change of $\delta m_F = \pm 1$ and imparting a momentum of $\pm 2k_L$, where q_x denotes the quasimomentum. The geometry and wavelength of the Raman field determine the natural units of the system: the single photon recoil momentum $k_L = \frac{2\pi}{\lambda_R}\sin(\theta/2)$, with λ_R the wavelength of the Raman laser and θ the relative angle between the Raman beams, and its associated recoil energy $E_L = \frac{\hbar^2 k_L^2}{2m}$.

After rotating to a frame at frequency ω_Z and a rotating wave approximation, the

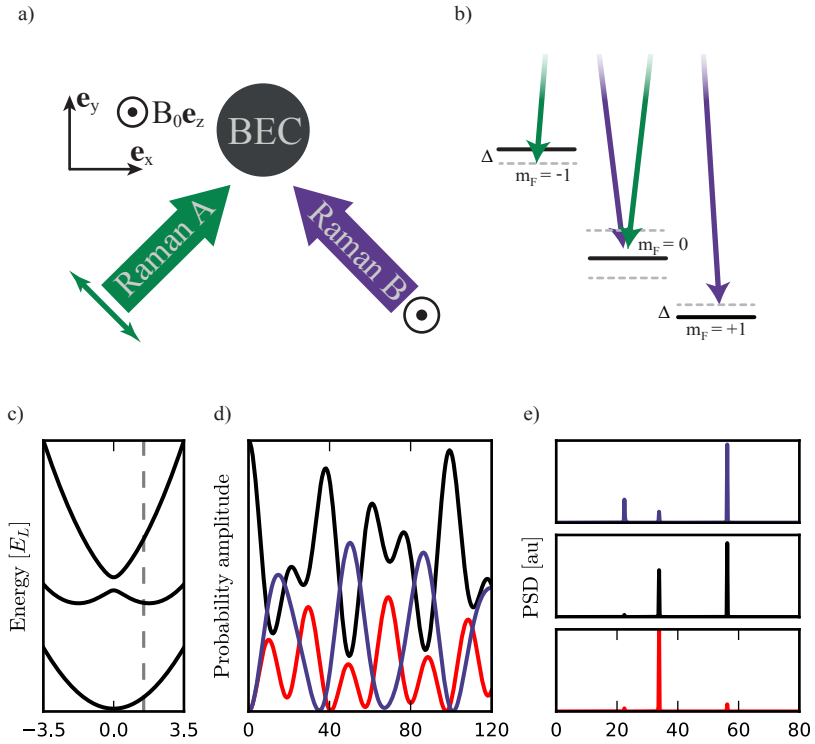

Figure 1. **c)** SOC dispersion of a spin-one system with quadratic Zeeman shift of $9E_L$ and Raman coupling $\Omega_0 = 12E_L$, initially prepared at a momentum $k_x = 2k_L$. **d)** Probability amplitude of measuring the atoms in the state $|m_F = -1,\ q_x = q_x + 2k_L\rangle$ (red), $|m_F = 0,\ q_x = q_x\rangle$ (black), and $|m_F = +1,\ q_x = q_x - 2k_L\rangle$ (blue) as a function of Raman pulsing time. **e)** Fourier transform of the probability amplitude. The three peaks in the Fourier spectra correspond to the three relative energies in the SOC dispersion for the parameters described above.

kinetic and atom-light contributions of the Hamiltonian along the recoil direction are

$$\begin{aligned}\hat{H}_x =& \frac{\hbar^2\hat{q}_x^2}{2m} + \alpha_0\hat{q}_x\hat{F}_z + 4E_L\mathbb{I} + \frac{\Omega_R}{2}\hat{F}_x] \\ &+ (-\epsilon + 4E_L)(\hat{F}_z^2 - \mathbb{I}) + \Delta_0\hat{F}_z,\end{aligned} \tag{1}$$

where $\hat{F}_{x,y,z}$ are the spin-one matrices, $\alpha_0 = \frac{\hbar^2 k_L}{m}$ is the SOC strength, and $\Omega_R \propto E_A^\star E_B$ is the Raman coupling strength which is proportional to the field intensity. We have also defined the direction of the $\mathbf{e}_x$ axis to be parallel to k_L.

Figure 1c shows a typical band structure of a SOC system as a function of quasimomentum that results of diagonalizing the Hamiltonian $\hat{H}_x$ for a negative quadratic Zeeman shift $|\epsilon| > 4E_L$. The ground state band is pushed to lower energy with respect to the higher excited bands, and it can be well described by a harmonic potential as there are no crossings with the higher bands.

1.1. Fourier spectroscopy of spin-orbit coupled atoms

We can directly measure the dispersion relation of a system of spin-one, spin-orbit coupled atoms by studying the time evolution of the Hamiltonian.

We start with bare atoms in the $|m_F = 0,\ k_x\rangle$ state. When a Raman field is suddenly turned on, the initial state is projected into the Raman dressed state basis, and continues to evolve $|m_F = 0, q_x\rangle \rightarrow \sum_{i=1}^{3} c_i e^{i\omega_i t}|\psi_i\rangle$, where $\omega_i = E_i/\hbar$ are the angular frequencies associated to the dressed state energies and $|\psi_i\rangle$, the dressed eigenstates, are linear combinations of $|m_F = 0,\ q_x = k_x\rangle$ and $|m_F = \pm 1,\ q_x = k_x \mp 2k_L\rangle$. We then suddenly turn off the Raman field and image the atoms, which projects the system back into the bare basis $|m_F = 0,\ q_x = k_x\rangle$, $|m_F = \pm 1,\ q_x = k_x \mp 2k_L\rangle$. The probability amplitude of measuring atoms in an m_F state after evolving for a time t oscillates at frequencies given by the difference in the dressed state energies $P_{m_F}(t) = \sum_{i \neq j} 2c_{ij} \cos((\omega_i - \omega_j)t)$.

The Fourier spectroscopy technique relies in directly measuring the probability amplitude as a function of time and extracting the relative energies of the system using a Fourier transform, as shown in figure 2d, e.

The method described above so far only allows us to measure relative energie. To recover the dispersion relations we must add a known energy reference by measuring the effective mass $m^\star = \hbar^2[\frac{d^2E(k_x)}{dk_x}]^{-1}$ of the nearly quadratic lowest branch of the dispersion, and then shifting the measured frequencies accordingly.

We can map the full spin and momentum dependent band structure of the SOC system by repeating this procedure for different initial momentum states, however, non-moving atom cloud in the laboratory reference frame dressed by a laser field with non-zero detuning is equivalent to a moving cloud with a resonant field in the cloud reference frame as can be explicitly seen in the Eq. 1. The detuning term $\Delta_0 \hat{F}_z$ and the momentum term $\alpha_0 \hat{q}_x \hat{F}_z$, have the same effect in the relative energies. All the energies are shifted when the associated with the transformation between reference frames, which gets canceled when we look at the energy differences. Therefore, for the purpose of our experiments, momentum and detuning are equivalent up to a numerical factor: $\Delta_0/E_R = 4q_x/k_R$.

1.2. Spectroscopy of periodically driven SOC system

A time-domain based spectroscopy is ideally suited to study the energy spectrum of more complex time dependent systems. A particularly interesting case is that of periodically driven systems [7, 10, 11], which are well suited for engineering and tuning Hamiltonians, as they can be described by effective coupling terms that arise from averaging the fast dynamics of the system.

We will study a spin-1 SOC system that is coupled by a multiple frequency Raman field, as shown in Fig 2. The interference of the multiple frequencies leads to a periodic amplitude modulation in the field and an effective Floquet Hamiltonian with a tunable

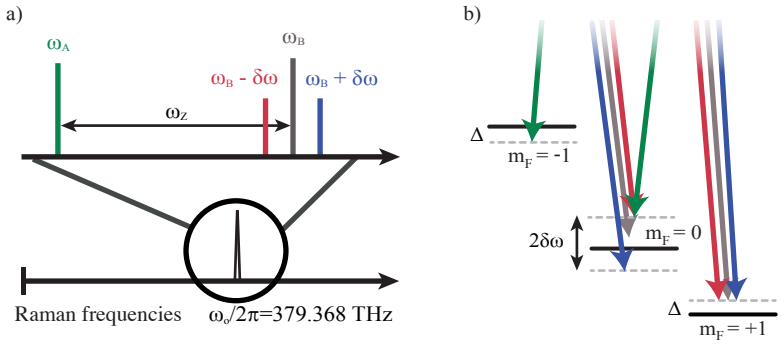

Figure 2. We use a multiple frequency Raman beam with up to 3 frequencies that gives rise to a system with tunable spin-orbit coupling. **(a)** Frequency components in each Raman beam **(b)** The combination of a blue and red sideband are at four photon resonance between the $|m_F = +1\rangle$ and $|m_F = -1\rangle$ state and there are two possible paths to couple these states.

SOC strength term [7].

We add two sidebands to one Raman beam at angular frequencies $\omega = \omega_L + \omega_Z + \Delta_0 \pm \delta\omega$. The Hamiltonian in Eq.1 remains unchanged, except for the coupling strength that takes the form $\Omega_R(t) = \Omega_0 + \Omega\cos(\delta\omega t)$. Our periodically driven system is well described by Floquet theory. The eigenstates are of the form $|\Psi_{\epsilon_m}(t)\rangle = \sum_{l=-\infty}^{+\infty} e^{-i(\epsilon_m - l\delta\omega)t}|\psi_{\epsilon_m,l}(t)\rangle$ where $|\psi_{\epsilon_m,l}(t)\rangle$ are time-periodic states and $\epsilon_m + l\delta\omega$ are the quasi-energies.

Rather than solving the full Floquet problem, we calculate the propagator for one driving period $T = 2\pi/\delta\omega$ and define an effective, time-independent, Hamiltonian $e^{iT\hat{H}_{eff}}$, with $\delta\omega \gg 4E_L$. This effective Floquet Hamiltonian retains the form of Eq.1 with renormalized coefficients, and an additional term that couples the $m_f = -1$ and $m_f = +1$ states:

$$\begin{aligned}\hat{H} =& \frac{\hbar^2\hat{k}^2}{2m} + \alpha\hat{k}\hat{F}_z + 4E_L\mathbb{I} + \frac{\Omega_0}{2}\hat{F}_x \\ &+ \frac{\tilde{\Omega}}{2}\hat{F}_{xz} + (\tilde{\epsilon} + 4E_L)(\hat{F}_z^2 - \mathbb{I}) + \tilde{\Delta}\hat{F}_z,\end{aligned} \tag{2}$$

where $\alpha = J_0(\Omega/2\delta\omega)\alpha_0$, $\tilde{\Omega} = \frac{1}{4}(\epsilon + 4E_L)(J_0(\Omega/\delta\omega) - 1)$, $\Delta = J_0(\Omega/2\delta\omega)\Delta_0$, and $\tilde{\epsilon} = \frac{1}{4}(4E_L - \epsilon) - \frac{1}{4}(4E_L + 3\epsilon)J_0(\Omega/\delta\omega)$, and J_0 the zero order Bessel function of the first kind.

When the quadratic Zeeman shift and the driving frequency are large compared to the recoil energy $|\epsilon|, \delta\omega > 4E_L$, the Hamiltonian in Eq. 2 can be approximated by an effective spin 1/2, SOC system,with tunable spin-orbit coupling: the state $|m_F = +1,\ q_x = k_x - 2J_0(\Omega/2\delta\omega)k_R\rangle$ is coupled to the $|m_F = -1,\ q_x = k_x + 2J_0(\Omega/2\delta\omega)k_R\rangle$

with coupling strength $\Omega' = \tilde{\Omega} + \hbar\Omega_0^2/2\tilde{\epsilon}$ [12]. In order to get a full control over the SOC gap and the SOC strength, we need to have control over the parameters $\delta\omega$, Ω and Ω_0.

The effective Hamiltonian correctly captures the energies within one Floquet manifold, however, if the coupling strength becomes comparable to the driving frequency Ω_0, $\Omega \geq \delta\omega$, the RWA breaks down and the counter-rotating terms can not be ignored. The signature of this is the appearance of higher frequency Fourier components in the probability amplitude, spaced by $\delta\omega$ from the lowest three energy levels. We expect the band structure from this type of system to be more complex, but easily interpreted by understanding the periodically repeating structure of the Floquet quasi-energies.

2. Experiment

We measured the SOC dispersion for various values of Ω and Ω_0: (i) A time independent spin-orbit coupled system, $\Omega_0 \neq 0$ and $\Omega = 0$, (ii) for a periodically driven spin-orbit coupled system with no DC offset $\Omega \neq 0$ and $\Omega_0 = 0$, and (iii) A time periodically driven spin-orbit coupled system with a DC offset $\Omega \neq 0$ and $\Omega_0 \neq 0$.

2.1. Spectroscopy experimental sequence

We start our experiments with a Rb^{87} Bose-Einstein condensate [13] (BEC) with $N \approx 4 \times 10^4$ atoms in the $|F = 1, m_F = 0\rangle$ state, confined in a 1064 nm crossed optical dipole trap, with trapping frequencies $(\omega_x, \omega_y, \omega_z) = 2\pi(42(3), 34(2), 133(3))$ Hz. We break the degeneracy between the m_F magnetic sub-levels by applying a 17.0556 G bias field along the z axis, which produces a Zeeman splitting of 12 MHz. The quadratic Zeeman shift that lowers the energy of the $|F = 1, m_F = 0\rangle$ state by 20.9851 kHz. We adiabatically prepare our BEC in the $|m_F = 0\rangle$ by slowly ramping the bias field while applying a 12 MHz radio-frequency field. We generate spin-orbit coupling between the magnetic sub levels with a pair of intersecting, cross-polarized Raman beams, with wavelength $\lambda_R = 790.024nm$ propagating along $\mathbf{e}_x + \mathbf{y}$ and $\mathbf{e}_x - \mathbf{e}_y$ as shown in Fig. 1a. The frequency of the beams is controlled by two acusto-optic modulators (AOMs), one of which is driven at multiple frequencies. When on resonance, the laser frequencies satisfy the condition $\omega_A - \omega_B = \omega_A - \frac{\omega_{B+} + \omega_{B-}}{2} = \omega_Z$, and we change the Raman detuning Δ_0 by keeping the magnetic field constant and changing the value of the frequency ω_A.

We measure Rabi oscillations at fixed Δ_O by pulsing the Raman beams for time intervals of up to 900 μs. The pulsing times and number of points are chosen so that the bandwidth is comparable or larger than the highest frequency system while maximizing resolution, with the constriction that we start observing decoherence in the oscillations after 900 μs. For the time independent SOC case (i) we chose to pulse for 120 different time intervals, and for the periodically driven SOC cases (ii, iii) we pulse for 180 time intervals. After pulsing the Raman we release our atoms from the optical dipole trap and let them fall for a $21ms$ time of flight (TOF) time before and apply a spin-dependent force using magnetic field gradient. Our absorption images reveal the atoms

spin and momentum distribution, from which we can extract the probability amplitudes by counting the fractional number of atoms in each spin and quasimomentum state. We repeat this procedure for values of Raman detuning within the interval $\pm 12E_L$ which corresponds to quasimomentum values $\pm 3k_L$.

The time dependent SOC measurements additionally required phase stability between the 3 frequency components in the Raman B field. All the relative phases are set to zero as it maximizes the effective couplings Ω and Ω_0 for a given Raman field intensity. For a more detailed discussion of the effect of the relative phases in the Hamiltonian see the Appendix section (?).

2.2. Effective mass measurement

We measure the effective mass of the Raman dressed atoms by adiabatically preparing our BECs in the lowest eigenstate and inducing dipole oscillations. The effective mass $m^\star$ of the dressed atoms is related to the bare mass m and the bare and dressed trapping frequencies ω and $\omega^\star$ by the ratio $m^\star/m = \sqrt{\omega^\star/\omega}$. We prepare our system in the $|m_F = 0,\ k_x = 0\rangle$ and adiabatically turn on the Raman in ~ 10 ms while also ramping the detuning to a non-zero value, around $0.5E_R$. We then change the magnetic field away from resonance, shifting the minima in the ground state energy away from zero quasi-momentum. We then suddenly bring the field back to resonance which excites the dipole mode of our optical dipole trap. To measure the bare state frequency, we use the Raman beams to initially excite the dipole mode of the trap but subsequently turn them off (~ 1 ms) and let the BEC oscillate in the unmodified dipole potential.

For this set of measurements we modified our trapping frequencies to $(\omega_x, \omega_y, \omega_z) = 2\pi(35.9, 32.5, xx)$ Hz so that they were nominally symmetric along the $x - y$ plane.

2.3. Magnetic field stabilization

We stabilized the magnetic field and measured fluctuations about the desired set point by applying a pair of microwave pulses to transfer a small fraction of atoms into $5^2\mathrm{S}_{1/2}$ $F = 2$ state which we can non destructively image in-situ.

We first prepare our BEC in the $|F = 1, m_f = 0\rangle$ state and apply a 17.0556 G bias filed along the z axis. We then apply a pair of $250\mu s$ microwave pulses close to $6.83GHz$ that transfers about 10% of the atoms into the $F = 2$ manifold. The pulses were detuned by ± 2 kHz from the $|F = 1, m_F = 0\rangle \leftrightarrow |F = 2, m_F = 1\rangle$ transition and were spaced in time by $1/2 \times 60s$. We image the atoms transfered into $|F = 2, m_F = 1\rangle$ without disturbing atoms in $F = 1$ since the imaging light is very detuned. The imbalance in the number of atoms transferred by each pulse gives us a 4 kHz wide error signal that we use both to feed forward our bias coils for active field stabilization, and also to keep track of the magnetic fields at each shot. We trigger our sequence to the line and both the microwave and Raman pulses are timed at integer periods of 60 Hz and performed at the zero-derivative point of the 60 Hz curve in order to minimize additional magnetic field fluctuations

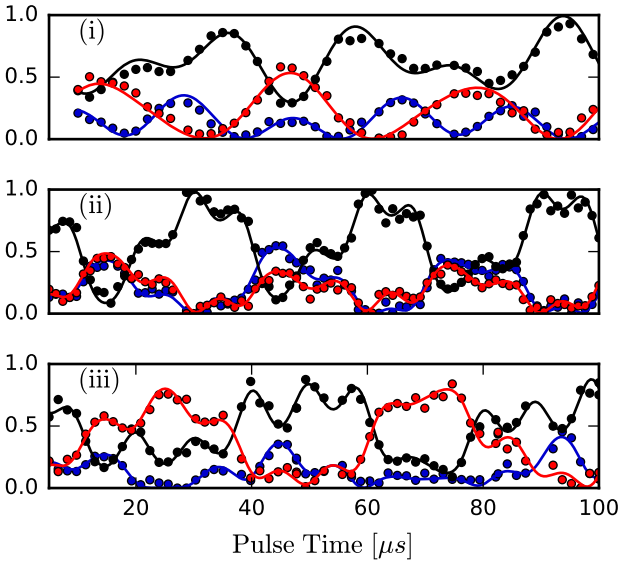

Figure 3. Time evolution of the BEC for Raman pulsing times between 5 and 10 μs, for different spin orbit coupling regimes: **(i)** $\Omega_0 = 9.9E_L$, $\Omega = 04$, $\Delta = 5.8E_L$, **(ii)** $\Omega_0 = 0$, $\Omega = 8.6E_L$, $\Delta = -0.7E_L$, and **(iii)** $\Omega_0 = 1.5E_L$, $\Omega = 8.4E_L$, $\Delta = -4.7E_L$

3. Results

We mapped the three band structure of our spin-orbit coupled atoms. We fit the data to the Hamiltonian in Eq. 1 with Δ_0 and Ω_R as the only free parameters. The fitted values agree well with microwave and Raman power calibrations. Figure 3 shows representative traces for the time evolution of our system for the three cases outlined above. The Raman coupling strength remained nominally constant throughout our measurements.

Since the Raman coupling strength Ω, Ω_R is comparable to the separation between the Floquet manifolds $\delta\omega$, the time evolution shows higher frequency components for the driven SOC measurements (cases (ii) and (iii)), that correspond to the Floquet quasi-energy spectrum,

We use a non-uniform fast Fourier transform algorithm (NUFFT) to obtain the power spectral density since our data points are not evenly spaced in time due to experimental uncertainties. Figure 4 shows the power spectral density (PSD) of the time evolution of each m_F state. Each vertical cut is normalized to the highest peak of the three spin states.

For the second and third rows we notice peaks at constant frequencies of $\delta\omega$ and $2\delta\omega$, independently of the Raman detuning, and a structure that is symmetric about the frequencies $2\pi f = \delta\omega/2$ and $2\pi f = \delta\omega$ which can be interpreted as the atoms coupling to the neighboring Floquet manifolds.

The missing peaks in the PSD are due to dark states at $\Delta_0 = 0$. Since there are eigenstates of the Raman dressed Hamiltonian that never get populated, the time

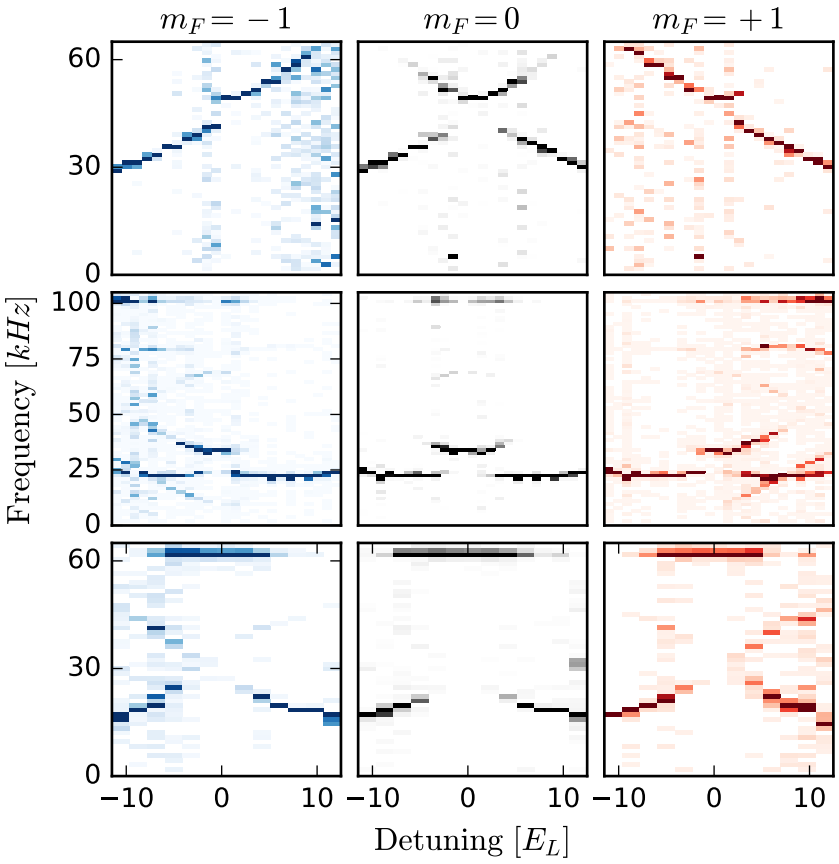

Figure 4. Power spectral density of the experimentally measured probability amplitudes for for different spin orbit coupling regimes: **(i)** $\Omega_0 = 9.9E_L$, $\Omega = 04$, $\Delta = 5.8E_L$, **(ii)** $\Omega_0 = 0$, $\Omega = 8.6E_L$, $\Delta = -0.7E_L$, and **(iii)** $\Omega_0 = 1.5E_L$, $\Omega = 8.4E_L$, $\Delta = -4.7E_L$

evolution of the system does not have the frequency components related to the missing eigenstates.

The effective mass was extracted by comparing the sloshing frequencies of the atoms in the dipole trap to the Raman dressed ones. fitted sinusoids to the sloshing motion of our atoms in the dipole trap and extracted the frequency of oscillation.

$$\hat{H}_\perp = \frac{1}{2m^\star}k_x^2 + \frac{1}{2m}k_y^2 + \frac{m}{2}[\omega_{x'}^2 x'^2 m + \omega_y'^2 y'^2] \tag{3}$$

with $\mathbf{e}_{x'} = \frac{\mathbf{e}_x + \mathbf{e}_y}{\sqrt{2}}$ and $\mathbf{e}_{y'} = \frac{\mathbf{e}_x - \mathbf{e}_y}{\sqrt{2}}$. For $\omega_{x'} = \omega_{y'}$ a simple rotation yields a trapping frequency along the Raman direction $\omega_x = \sqrt{\omega_x^2 + \omega_y^2}$. Figure 5 shows the dipole oscillations along the $\mathbf{e}_{x'}$ and $\mathbf{e}_{x'}$ directions for the three different coupling regimes we are studying, as well as the bare state motion.

We can obtain the characteristic dispersion of a SOC system after subtracting the effective mass, as can be seen in Figure 6. The measured bands are in good agreement with the eigenvalues calculated from Floquet theory.

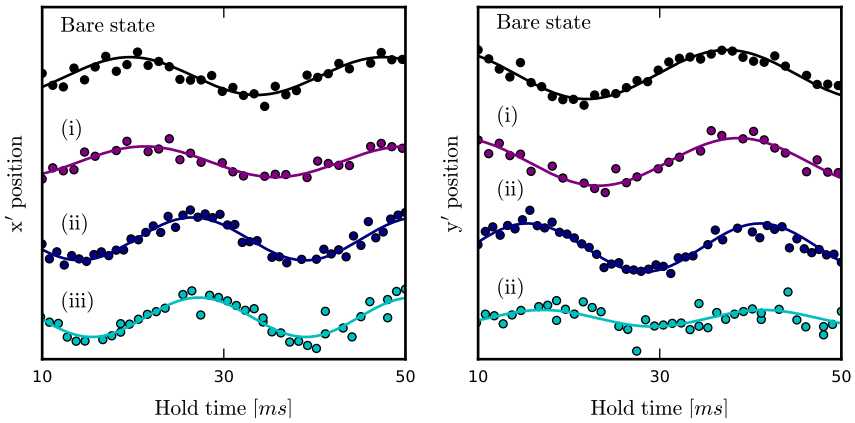

Figure 5. Oscillation of the BEC in the dipole trap along the directions $\mathbf{e}_{x'}$ and $\mathbf{e}_{y'}$ defiend by the propagation of the dipole tap beams. The traces have been shifted so that it is easier to appreciate the change in the motion for each coupling regime.

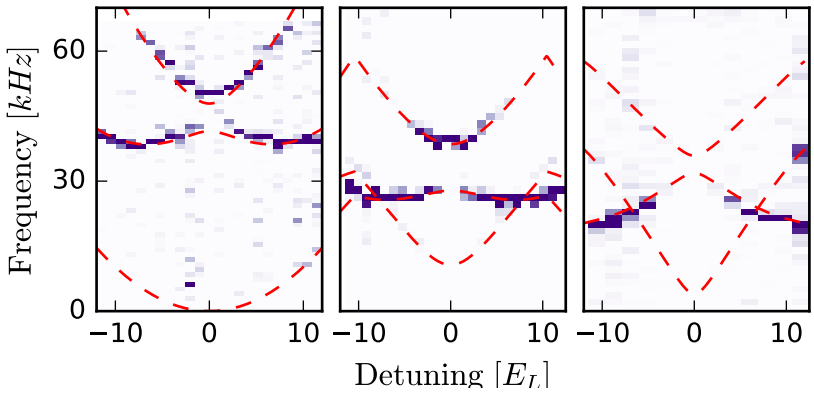

Figure 6. This figure needs some love but this is more or less the idea. Only the first panel has the effective mass substracted, other 2 are energy differences. I was thinking of maybe making the theory lines thicker to include uncertainties.

4. Discussion

Heating due to scattering of spontaneously emitted photons is always present in our system. It is also well known that heating is present in periodically driven systems, and while it can be minimized by increasing the driving frequency, it in exchange requires more Raman power to tune the spin-orbit coupling strength. The time scales of our pulsing experiments never exceeded 900 μs which is small compared to the lifetime of our system.

In conclusion, we can measure the spin and momentum dependent dispersion relation for a spin-1 spin-orbit coupled BEC using a newly developed Fourier spectroscopy technique. When used to study periodically driven systems, we are able tp see a rich spectrum that arises from the Floquet quasi-energies. This method can be applied generically to any effective three level system with a quadratic branch in the

spectrum. This technique might prove particularly useful to probe the spin-resolved energy dispersion of atoms in the presence of Rashba spin-orbit coupling using newly proposed schemes to generate this type of coupling without the use of excited states [14] and could lead to a better understanding of new topological materials.

[1] Lindner N H, Refael G and Galitski V 2011 *Nature Physics* **7** 490–495 ISSN 1745-2473 URL http://www.nature.com.proxy-um.researchport.umd.edu/nphys/journal/v7/n6/full/nphys1926.html
[2] Radić J, Natu S S and Galitski V 2015 *Physical Review A* **91** 063634 URL http://link.aps.org/doi/10.1103/PhysRevA.91.063634
[3] Yoshimura B, Campbell W C and Freericks J K 2014 *Physical Review A* **90** 062334 URL http://link.aps.org/doi/10.1103/PhysRevA.90.062334
[4] Wang L, Zhang H, Zhang L, Raithel G, Zhao J and Jia S 2015 *Physical Review A* **92** 033619 URL http://link.aps.org/doi/10.1103/PhysRevA.92.033619
[5] Cheuk L W, Sommer A T, Hadzibabic Z, Yefsah T, Bakr W S and Zwierlein M W 2012 *Physical Review Letters* **109** 095302 URL http://link.aps.org/doi/10.1103/PhysRevLett.109.095302
[6] Dalibard J, Gerbier F, Juzeliūnas G and Öhberg P 2011 *Reviews of Modern Physics* **83** 1523–1543 URL http://link.aps.org/doi/10.1103/RevModPhys.83.1523
[7] Jiménez-García K, LeBlanc L, Williams R, Beeler M, Qu C, Gong M, Zhang C and Spielman I 2015 *Physical Review Letters* **114** 125301 URL http://link.aps.org/doi/10.1103/PhysRevLett.114.125301
[8] Lan Z and Öhberg P 2014 *Physical Review A* **89** 023630 URL http://link.aps.org/doi/10.1103/PhysRevA.89.023630
[9] Campbell D L, Price R M, Putra A, Valdés-Curiel A, Trypogeorgos D and Spielman I B 2015 *arXiv:1501.05984 [cond-mat, physics:physics]* ArXiv: 1501.05984 URL http://arxiv.org/abs/1501.05984
[10] Eckardt A, Weiss C and Holthaus M 2005 *Physical Review Letters* **95** 260404 URL http://link.aps.org/doi/10.1103/PhysRevLett.95.260404
[11] Goldman N and Dalibard J 2014 *Physical Review X* **4** 031027 URL http://link.aps.org/doi/10.1103/PhysRevX.4.031027
[12] L J LeBlanc M C B 2013 *New Journal of Physics* **15** ISSN 1367-2630
[13] Lin Y J, Perry A R, Compton R L, Spielman I B and Porto J V 2009 *Physical Review A* **79** 063631 URL http://link.aps.org/doi/10.1103/PhysRevA.79.063631
[14] Rashba realization: Raman with RF - IOPscience URL http://iopscience.iop.org/article/10.1088/1367-2630/18/3/033035/meta

5. Appendix A

5.1. Effective SOC Hamiltonian

Maybe I will put a more detailed derivation of the theory here, not sure.